IEEE Access
Multidisciplinary | Rapid Review | Open Access Journal

Received April 21, 2019, accepted May 6, 2019, date of publication May 15, 2019, date of current version May 30, 2019.

Digital Object Identifier 10.1109/ACCESS.2019.2917145

Pattern Reconfigurable Cubic Slot Antenna

SOUREN SHAMSINEJAD[1], (Student Member, IEEE), NABIL KHALID[1], (Student Member, IEEE), FATEMEH M. MONAVAR[1], (Student Member, IEEE), SHILA SHAMSADINI[1], (Senior Member, IEEE), RASHID MIRZAVAND[1,2], (Senior Member, IEEE), GHOLAMREZA MORADI[2], (Senior Member, IEEE), AND PEDRAM MOUSAVI[1], (Senior Member, IEEE)

[1]Intelligent Wireless Technology Laboratory, University of Alberta, Edmonton, AB T6G 2R3, Canada
[2]Electrical Engineering Department, Amirkabir University of Technology, Tehran 15914, Iran

Corresponding author: Nabil Khalid (nkhalid1@ualberta.ca)

This work was supported by the NSERC-AITF Industrial Research Chair Program.

ABSTRACT In this paper, a cubical 3D folded slot antenna array with reconfigurable radiation pattern is reported. The proposed antenna is capable of switching between omnidirectional and broadside radiation pattern. The hollow nature of the design is beneficial for applications such as wireless sensor networks, where electronic circuits can be installed inside the antenna, producing a small overall packaged device. A robust feeding mechanism is also proposed that utilizes electronic switches to shift between the two offered radiation patterns, namely, omnidirectional and directional. A cubic prototype at 2.4 GHz having a gain of 2.85 dBi and 4.2 dBi along with input matching bandwidth of 21% and 2.7%, for the omnidirectional and broadside radiation case, respectively, has been presented. Whereas, the final antenna dimensions are $39.5\times39.25\times30$ mm^3. 3D and printable nature of the architecture makes the antenna a good candidate for the industry.

INDEX TERMS 3D printable antenna, reconfigurable antenna, cubic antenna, slot array.

I. INTRODUCTION

Wireless sensor networks (WSNs) has gained significant attention in multitude of applications requiring monitoring of certain important parameters such as temperature, humidity, luminance, gas etc. This information helps in performing certain tasks more effectively, resulting in improved user experience, such as at home, in industry automation or even body care [1]–[3]. Antenna in a WSN is one of the most vital component as its limitation, such as low gain and coverage area, can highly limit the performance of the sensor. A major engineering milestone would be to design an antenna that receives in all directions while providing maximum gain in any required direction. An antenna-in-package with conductive body and slot for radiation [4], offers a promising solution as it can be engineered to have reconfigurable radiation patterns. Furthermore, it provides an opportunity to place electronic circuits inside the package and thus protecting them from harsh environmental conditions along with strong RF interferences or electron bombardment in the space.

Sensory nodes can be installed in rural areas with strong direct link or urban areas with dominant multipath propagation, due to presence of obstacles. As long as the nodes are installed at the same height, in both cases, the distribution of angle of arrivals is concentrated around horizon. Hence an omnidirectional radiation pattern in the azimuth plane that offers enough gain in the plane would be a great choice to connect the nodes. However, usually a sky communication link to the gateway or base station installed in tall tower, a drone or even a satellite, where most of the signal is received from broadside, demands a different radiation pattern. Hence, employing a reconfigurable antenna with capabilities of switching to directional radiation pattern can serve the purpose.

A lot of research has been conducted on investigating pattern reconfigurable antennas [5]–[11]. A good example is the research carried on developing reconfigurable antennas for WLAN. For example, in [5], rhombus-like patch antennas in an array with parasitic elements along with PIN

The associate editor coordinating the review of this manuscript and approving it for publication was Kwok L. Chung.

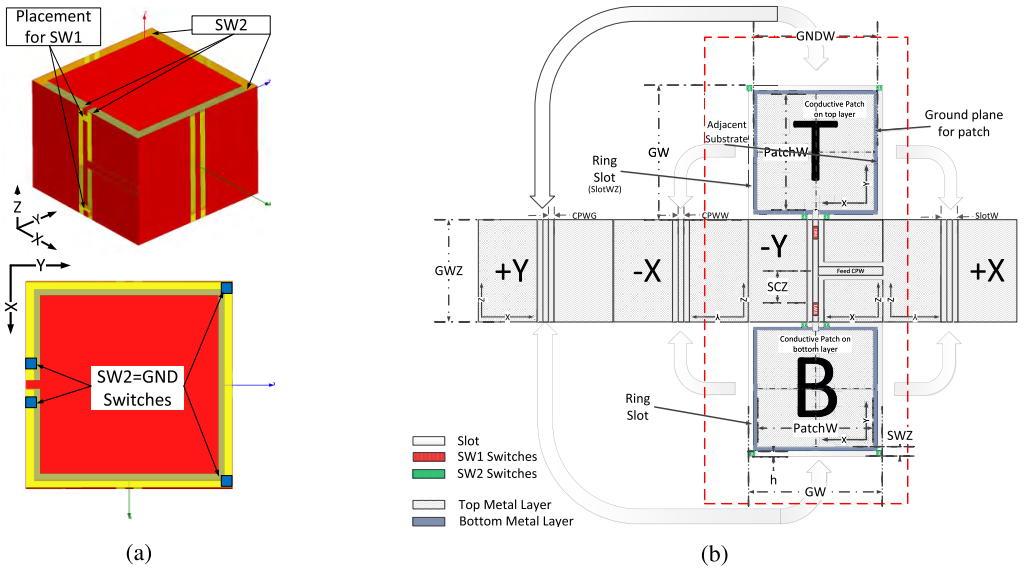

FIGURE 1. Proposed antenna (a) isometric view (upper figure) and Top view (bottom figure) (b) Flattened view of cubic antenna (T and B represents Top and Bottom faces, respectively. Arrows indicate the edges connected when in cubic form).

diodes as RF switches, are used to design an antenna having reconfigurable radiation pattern at 5.2 GHz. Similarly, a planar antenna array with PIN diodes is proposed in [6] that utilizes L-shaped quarter-wavelength slot at 2.4 GHz. Moreover, in [7], a planar antenna that can be configured to generate omnidirectional or directional radiation pattern at 3.8 GHz, is proposed. 3D folded slot antennas are employed in [8] and [9] to design antenna-in-packages whose inner space can be used for installing transceiver circuits. However, very little research is done on reconfigurable 3D antennas. In [12], a cubic slot antenna is proposed that uses PIN diodes to short-circuit the slots and provide reconfigurability. This design, however, is heavily influenced by the resonance inside the cube, which limits its use for housing electronics inside itself. A partitioned waveguide utilizing multimodes to achieve reconfigurability is presented in [13].

In this work, we propose a cubic antenna with reconfigurable radiation pattern which can switch between omnidirectional and directional radiation patterns. The contribution of the proposed work is threefold. First, the proposed antenna consists of a set of simple folded slots [14], that are wrapped around a cubic structure and act as radiator or transmission line, based on the mode of operation. Different modes are excited by changing states of switches, embedded in the antenna body, to generate the desired radiation pattern. In mode 1, constructive in-phase radiation from the walls produce a horizontally polarized omnidirectional radiation pattern in the azimuth plane. In mode 2, the antenna generates broadside radiation pattern with moderately high gain in the top or bottom faces of the cube using the respective simple patch antennas. Second, the flexible control of beams along with the proposed simple feeding mechanism, made possible through a CPW line, makes the proposed antenna a perfect candidate for low-cost 3D printed technologies. Third, the proposed design, allows the antenna to house electronics circuitry inside itself. The antenna operates at 2.4 GHz and is compatible with most of WSN technologies, such as Heart and ZigBee.

The remainder of this paper is organized as follows. In section II we discuss the details of our antenna design. While, section III is dedicated to antenna fabrication and comparing measurement and simulation results. Finally, the paper is concluded in section IV.

II. ANTENNA DESIGN

Our designed antenna integrates two different types of antennas, namely folded slot antenna and patch antenna. Therefore, to help reduce the design ambiguities, geometry aspects are discussed first. Following that, we discuss the working principle of our proposed antenna.

A. GEOMETRY

Structure of the proposed antenna is cube-shaped and thus it has six different faces, as shown in Fig. 1. The faces normal to z-axes are considered as top/bottom faces and consists of the patch antennas. While the side walls have folded slot antennas at every face. For excitation of the antenna, a coplanar waveguide (CPW) feed is used on the '-Y' face, which also enables the realization of the slots, Fig. 1. The patch on the top/bottom face of the cube has a width of *PatchW* surrounded by a small ring slot (*SlotWZ*), in between the patch and the substrate of the adjacent face. The ground plane beneath the patch has width of *GNDWW*. Whereas, on the side walls, the folded slots being used, have width of SlotWZ. Given their type, these antennas provide linear polarization. To enable different modes of operation, different

antennas are activated using switches namely, SW1 and SW2. The SW1 connects/disconnects the center signal line of the slot pairs to the top or bottom patches. Whereas, SW2 Connects patch ground plane to the rest of the cube body, when required.

B. ANTENNA OPERATION

1) MODE 1 (OMNIDIRECTIONAL PATTERN)

In this mode, all vertical slot pairs, on side walls of the cube, are excited in-phase to achieve constructive interference in the azimuth plane. This mode generates the desired omnidirectional radiation pattern. The operation of antennas in this mode can be explained by considering an array of four radiating elements in the XY-plane and spaced equally apart from each other and at distance GW/2 from the origin. Detailed treatment on similar antenna arrays can be found in [15]–[17]. Since all the slot antennas are oriented in different directions, it should be kept in mind that this peculiar behavior must be incorporated in the governing equations. A detailed derivation is shown in Appendix.

In order to produce a horizontally polarized omnidirectional radiation pattern, in-phase ϕ-polarized electric fields (red arrows) should be set up in the azimuth plane of the cubic antenna (Fig. 2). The resulting magnetic current distribution (blue arrows) is analogous to the magnetic current flow of rectangular slots placed on all four side walls (vertical faces) of the cube. This current configuration creates maximum electric field at the center of the slots, resulting in maximum gain in the azimuth plane. To ensure minimum radiation in top/bottom of the cube, the electric field should have nulls on these faces. As evident from Fig. 2, the continuation of currents to the top and bottom surfaces of the cube will cause out-of-phase electric fields which conclusively result in cancellation of radiation along these directions. As shown in Fig. 2, such a slot magnetic current/electric field configuration is easily achieved through wrapping a planar folded slot array around a cube. Given the fact that radiation needs to be minimized on top and bottom faces of the cube, and considering our final goal of reconfigurability, we have chosen two directive radiators on the top and bottom faces of the cube and kept them in non-radiating mode, when operating in mode 1 and thus avoid undesired radiation.

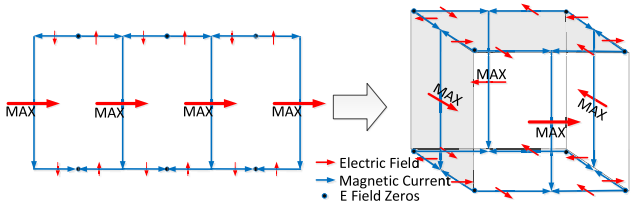

FIGURE 2. Designing antenna based on nominal magnetic current and electric field distribution of planar slot antenna (left) and folded slot antenna (right).

To ensure in-phase radiation from vertical slots on side walls of the cube, the length of the slots, along with the cube edge length were properly tuned and optimized. It was found that by having common mode slot pairs instead of single slots, radiation was balanced in all four slots, especially the slot on '-Y' face which is directly excited through a CPW line. Apart from balancing the radiation on all the four faces, the added conductor provides the opportunity to make the cube a reconfigurable antenna.

2) MODE 2 (DIRECTIONAL PATTERN)

In this mode, a directional radiation pattern in either top or bottom side can be generated. This is achieved by exciting only one patch antenna at a time, while, the other patch antenna is disconnected by turning off one of the two SW1. Moreover, the ground of the unused patch antenna is in-addition connected to the body of the cube using the SW2 switch to improve the directivity.

As the cube allows finite ground plane beneath the active patch antenna, various models were analyzed to study the effects of different ground plane sizes on the radiation pattern of the antenna. Initially, we modeled a patch antenna with finite ground plane. The final antenna was modeled after examining the five subsequent models shown in Table 1. The radiation parameters are compared in Fig. 3.

TABLE 1. Models of the patch antenna.

Model #	Description	Schematic
Model 1	Top patch with finite ground plane and substrate	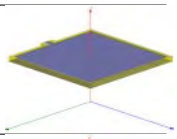
Model 2	Top patch with finite ground plane and extended substrate	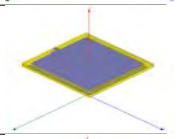
Model 3	Top patch with finite ground plane on a cubic substrate	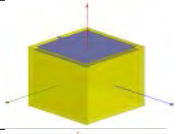
Model 4	Cubic antenna in Mode 2 without ground plane switches	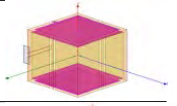
Reference	Cubic antenna in Mode 2	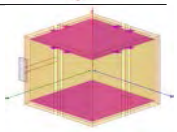
Model 6	Cubic antenna in Mode 2 with identical ground plane switches for the patch on the opposite side	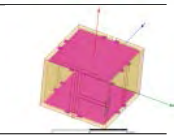

For conventional patches, we can see from Fig. 3 that front to back ratio, defined as the ratio of gain in front direction to the gain in the back direction, along with gain increases from model 1 to model 3. The substantial increase in the

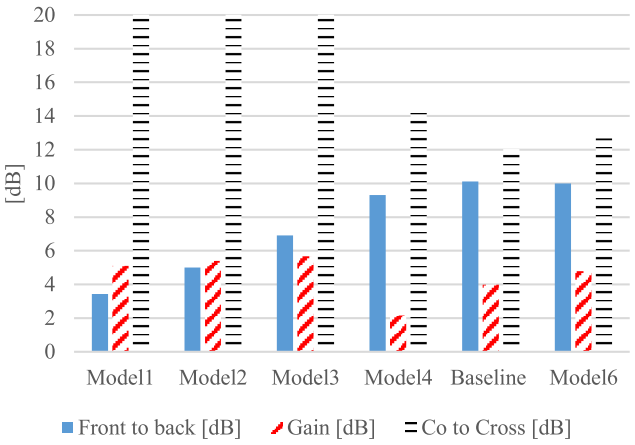

FIGURE 3. Radiation parameters of the models.

density of surface currents on the outer boundary of truncated ground plane in model 1 is responsible for low gain and rather poor front to back ratio as was previously proven in experimental [18] and numerical studies [19], [20]. Whereas, in model 2 and model 3, the substrate extended beyond the ground plane attenuates the undesired surface currents to a higher degree, resulting in higher gain and improved front to back ratio.

As we move on to building our cubic structure, model 3 is evolved to model 4 where cube surrounding walls are now covered with conductive surface. The appearance of metallic walls help to boost front to back ratio owing to cancellation of spurious radiations in the back-lobe regions, however, gain drops due to an increase in the level of cross polarized component (Fig. 3).

It can be seen in Fig. 3, how the values of front to back ratio in conventional patches of first three models are noticeably below those of reference model and model 6 which proves that the effect of diffraction from the edges of a finite ground plane is more pronounced in the back lobe region as already stated in [16]. However, such dramatic effects have been neutralized to a very good extent in our proposed antenna due to the presence of vertical cube walls and the fact that the bottom patch is disconnected and inactive in this mode. This proves how the alternate switching scheme for top and bottom patches serves to produce another key feature in our cubic antenna; the bottom patch could be perceived as a parasitic element which is not radiating by itself, but helps reduce the diffraction effects and hence lower the intensity of back lobe radiation. Similar effect was also observed in [21].

In our proposed model, the deactivation of parasitic (bottom) patch is done through a switch which can disconnect it from the surrounding vertical walls (extended ground plane in this mode) to guarantee that the patch performs as a director (as opposed to reflector when it is connected to the ground plane), which eventually helps the top patch antenna to radiate a more directional beam by suppressing undesired back lobes. The distance between active patch (radiator in this mode) and the parasitic patch is determined by the cube height which has a significant effect on antenna performance.

Next, we need to verify the feasibility of using the inner volume of the cube for the placement of electronic circuits. This can be verified by determining the locations where E-field is negligible. Results shown in Fig. 4, determined using full-wave EM simulation reveals that the E-field at the center of the cube is attenuated by 25 dB of its maximum. This suggests that a properly shielded circuit kept at the center will not interfere with the antenna fields and can be used to place the electronics circuit.

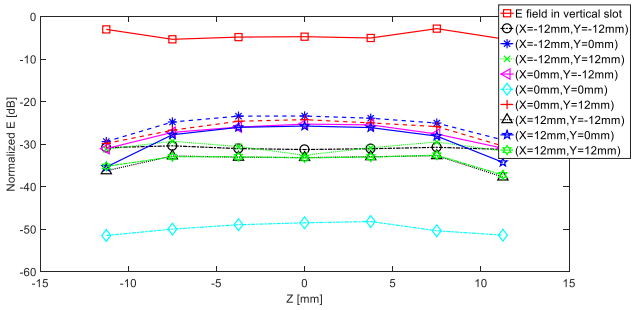

FIGURE 4. Comparison of E-field at different locations inside the antenna.

3) FEEDING STRUCTURE AND EXCITATION

In order to simplify the fabrication and offer better performance at potential high frequency applications by added shielding, the antenna is excited through a single layer CPW line placed on '-Y' face of the cube which is connected to an SMA in this prototype. The neighboring elements are excited through mutual coupling between the elements and act as the parasitic array elements, which reduces the complexity of the feeding structure.

The vertical slot pair placed on '-Y' face, switches between common mode (radiating slot mode) and differential mode (CPW transmission line mode), to achieve omnidirectional pattern in the azimuth plane in mode 1 and directional pattern towards top/bottom faces in mode 2, respectively. However, since a slot antenna exhibits a very high impedance at the center, CPW feeding becomes slightly challenging. Therefore, the antenna is fed at the center of '-Y' face, where the maxima of E-field occurs (Fig. 2). For mode 1 excitation, all the switches are kept in off state in order to observe folded slot antennas.

Electric fields shown by red arrows in Fig. 5 (a) illustrate how vertical slot pair is excited at even mode (common mode) through a horizontal CPW line. The width of conductor and gaps as well as transition from the feeding CPW line transverse to the radiating slot have been optimized and tuned for an omnidirectional radiation pattern and proper matching. On the other hand, in mode 2, the vertical slot pair on '-Y' face is excited in differential mode producing the E-field shown in Fig. 5 (b). In this configuration, one half of the slot pair acts as a transmission line connecting the input 50 Ω CPW and the active top/bottom antenna (selected by turning on one of the

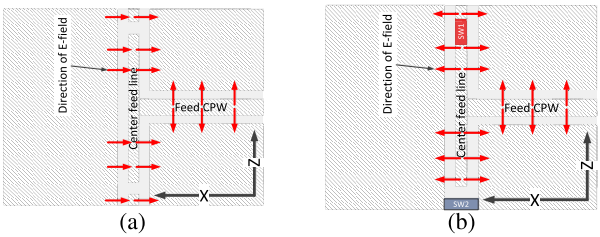

FIGURE 5. Antenna excitation modes using CPW transmission line, Slot pair in (a) common mode (b) differential mode.

two SW1s). While the other half acts as an open circuit stub, due to the fact that the other SW1 is off. This configuration inherently provides matching of 50 Ω input CPW feed line to high impedance differentially-excited slot pair on '-Y' face. As the patch is fed through a high impedance line, an inset feeding is not required. Moreover, the patch ground plane is connected to the body of the cube using SW2 switches.

Switches in our design play an important role in enabling reconfigurability. SW1 is used to connect/disconnect RF input line to the top or bottom patches, whereas, SW2 connect/disconnect patch ground planes to the cube body. RF switches are trigged through DC voltage running on RF lines, where an external bias Tee is used to combine RF and DC, together on the same line. This allows a single line to be used for biasing to generate any required mode. Table 2 shows required DC voltages at the input to switch between different modes. While schematic of our biasing network is shown in Fig. 6.

TABLE 2. Switch voltages for reconfiguring patterns.

Switching modes	Mode 1 3D folded slot	Mode 2 Top patch	Mode 2 Bottom patch
Radiation	Omnidirectional	Directional	directional
V_{dc}	$-1.4v < V_{dc} < 1.4v$	$V_{dc} > 1.4v$	$V_{dc} < -1.4v$
Top SW1	OFF	ON	OFF
Bottom SW1	OFF	OFF	ON
Top SW2	OFF	ON	OFF
Bottom SW2	OFF	OFF	ON

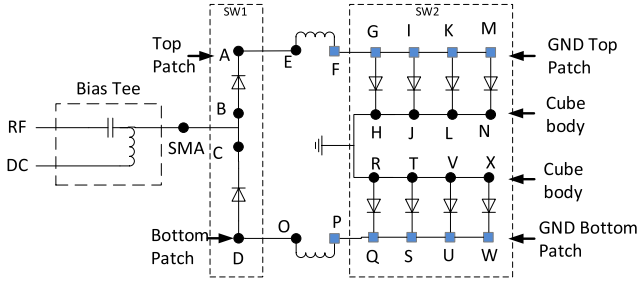

FIGURE 6. Schematic of the biasing network of the antenna.

C. PARAMETRIC VARIATION

To account for manufacturing tolerance in our proposed design, we study the variations of some key geometrical parameters and illustrate how strongly they would affect the antenna performance.

1) MODE 1 – EFFECT OF SLOT VARIATIONS

Widening the slot(s) on side walls of the cube increases the characteristic impedance. Fig. 7 represents change in input matching as the slot width on side walls vary within a 20% range. It was observed that the original slot width of 5 mm yields an omnidirectional pattern and resonance frequency of 2.44 GHz where its 10 dB input matching bandwidth covers the entire 2.4 GHz ISM band. Deviation within 10% still produced acceptable results, however, further changes deteriorates the omnidirectional pattern since it significantly disturbs the current distribution on the cube and moves the peaks and nulls of electric field from their ideal locations.

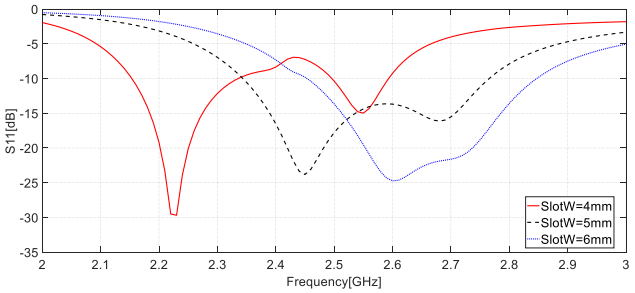

FIGURE 7. Effect of variation of slot width on reflection coefficient.

In mode 1, cube size determines the slot length and thus the antenna resonant frequency. The parameter GW was swept within a 50% range and its effect on directivity, and input matching was observed. Fig. 8 shows how the resonance frequency shifts as the length of the slot changes. Although, the antenna is still matched in the desired band, it was observed that the radiation pattern was no longer omnidirectional.

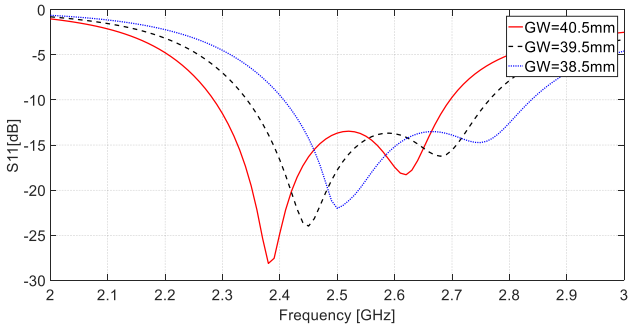

FIGURE 8. Effect of variation of slot length on reflection coefficient.

2) MODE 2 – EFFECT OF TOP/BOTTOM SLOT VARIATIONS

It was observed in the simulations that variations within 40% of width of Top/Bottom slot (SlotWZ) does not have a profound affect on the antenna performance. This is due to the fact that the variation of SlotWZ in terms of wavelength

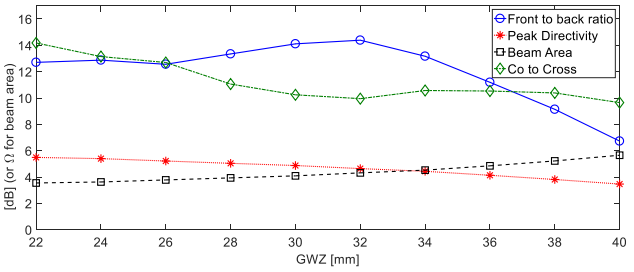

FIGURE 9. Antenna parameters variation versus cube height in mode 2.

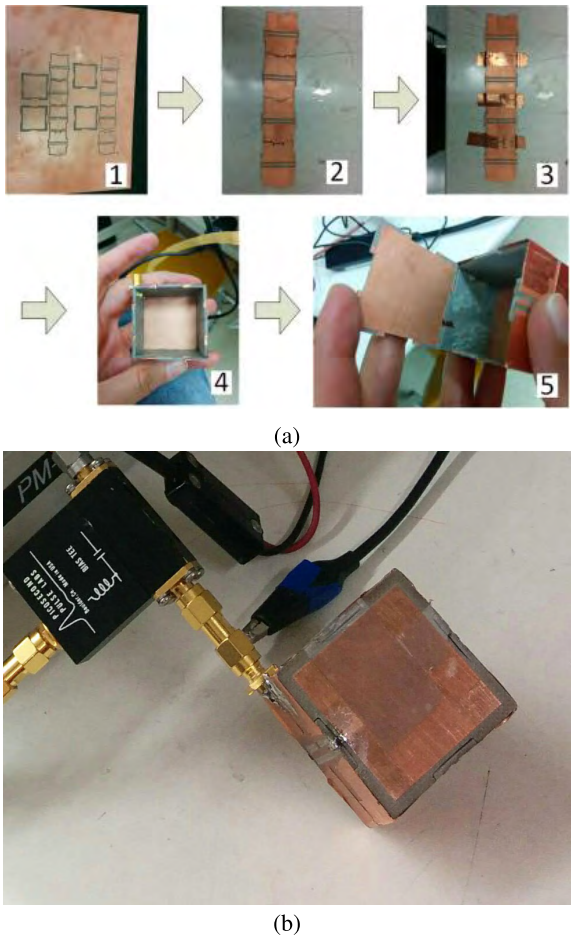

(a)

(b)

FIGURE 10. Fabricated reconfigurable antenna (a) design steps (b) testing with the biasing network.

TABLE 3. Dimensions of the antenna structure (designed on a substrate with relative permitivity of, $\epsilon_r = 2.97$ and height of, H = 1.55 mm).

Parameter	Description	Dimension (mm)
SlotW	Slot width (=CPWW+2×CPWG)	5
CPWG	Gap width	1.75
CPWW	Edge to edge distance between slot pairs	1.5
FeedCPWG	Gap in feeding CPW	0.2
FeedCPWW	Center line width in feeding CPW line	2
SlotWZ	Width of slot on top/bottom faces of cube	2.75
PatchW	Width of patch of top/bottom faces	34 ×34
GNDW	Width of patch ground plane	36.5
GW	Length and width of cube	39.5
GWZ	Height of cube	30
SCZ	Length of open circuit stub	13.5
V	Total Volume	39.5×39.5×30

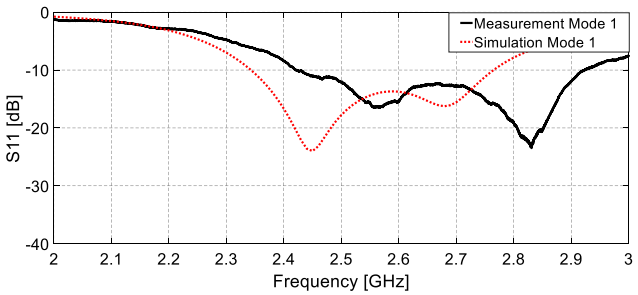

(a)

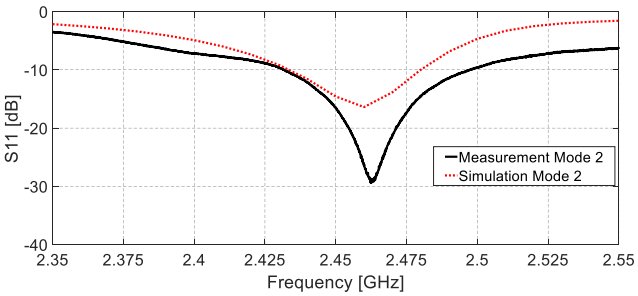

(b)

FIGURE 11. Input reflection coefficient, (a) mode1, (b) mode 2.

in dielectric is around $0.024\lambda_r$ to $0.052\lambda_r$, which does not vary surface waves in the substrate a lot and as a result the matching or radiation characteristics of the antenna remains almost the same, as expected.

Similarly, variations in cube height also does not affect the resonant frequency of the antenna as long as the feeding and matching network are intact. However, the distance between active or excited patch on one face and the patch that is not excited on the opposite face, together with the height of cube walls can affect the radiation properties of the antenna. This is due to the change of distance between the active elements and the coupled parasitic element.

By increasing the cube height, the amount of surface currents flow on the conductive walls of the cube increases which will result in some spurious radiation at undesired angles. This widens the beam area and leads to lower values of directivity and co to cross ratio as shown in Fig. 9.

We also notice that the front to back ratio is maximum for our chosen cube height of 30 mm, and it drops as GWZ is given a smaller or larger value. This is mainly because, there is an optimal distance for which all radiators contributing in the far field, including both active and parasitic elements, have out of phase radiations in the back-lobe region, which

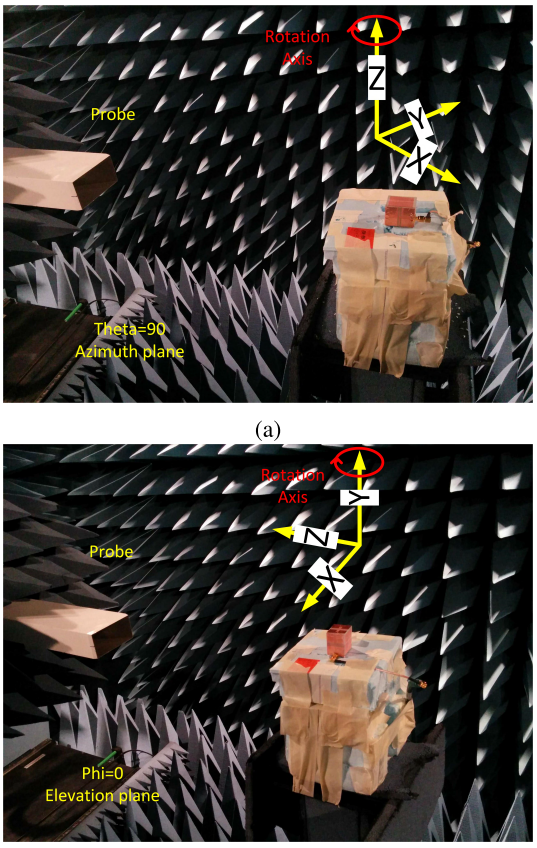

FIGURE 12. Radiation pattern measurement setup (a) XY plane (b) XZ plane.

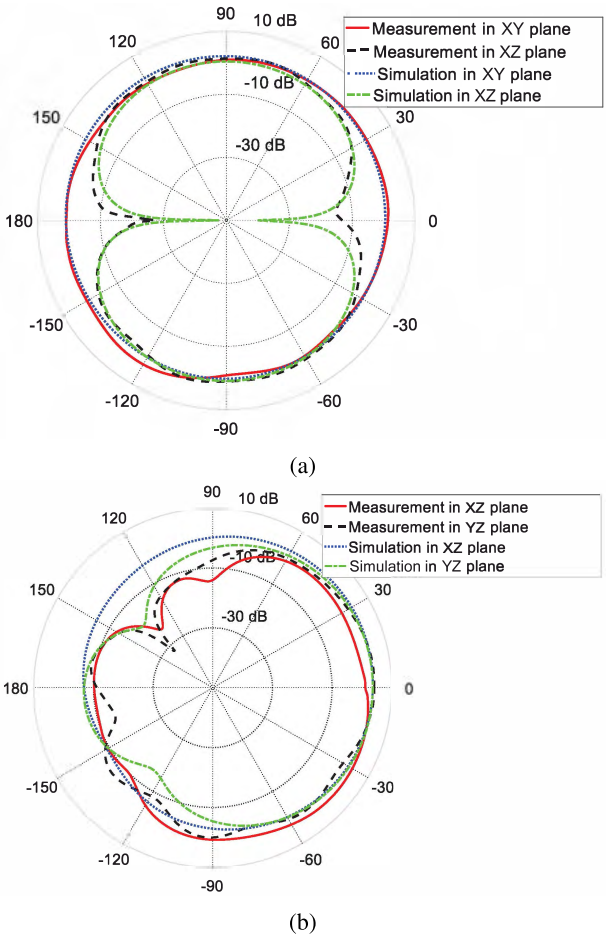

FIGURE 13. Realized gain from simulation vs measurement (0° corresponds to top face), (a) mode 1 (b) mode 2.

will result in back lobe suppression and maximum front to back ratio.

III. RECONFIGURABLE ANTENNA PERFORMANCE

The dimensions of the final circuit are shown in Table 3. Whereas, Fig. 10 shows the final reconfigurable antenna fabricated on an AD300 substrate.

Measured and simulated input reflection coefficients of antenna in mode 1 and mode 2 are compared in Fig. 11. Results in both the cases meet the requirements and antenna offers satisfactory performance around 2.4 GHz band with 504 MHz and 65 MHz bandwidth in mode 1 and mode 2, respectively. Slight discrepancy between simulation and measurement can be attributed to the manual fabrication of the antenna and presence of a high profile SMA connector on cube body.

In addition, antenna radiation pattern measurement setup is show in Fig. 12. The corresponding results are shown in Fig. 13 (a) and (b) for mode 1 and 2, respectively, which shows good agreement between simulated and measured results. The two modes were easily excited by simply using the switching network. Due to noticeable size of SMA connector on the antenna body and some undesired interaction with measurement setup (e.g. blockage effect caused by cables and metallic parts of the mast), there is slight deviation between the measured antenna radiation pattern and the simulation results. Furthermore, maximum realized gain was measured as 2.85 dBi and 4.2 dBi and efficiency of 84% and 80% for mode 1 and mode 2, respectively. These results satisfies our design goal of having a low gain omnidirectional pattern in the azimuth plane in mode 1, while a more directive broadside beam with higher gain in mode 2.

IV. CONCLUSION

In this paper, a novel 3D antenna structure for WSN applications has been presented. The antenna is reconfigurable and capable of generating both omnidirectional (mode 1) and patch-like (mode 2) radiation patterns. The former pattern was accomplished by using 3D folded slot array mapped on the cube side walls, whereas the latter was achieved through the excitation of patch antennas embedded on the top and bottom faces of the cube. The results show good agreement between measured and simulated gain and reflection coefficient. The antenna was matched at 2.44 GHz with maximum gain of 2.85 dBi and 4.2 dBi in mode 1 and mode 2,

respectively. The proposed antenna is a robust design and proves to be an excellent candidate for WSN applications.

APPENDIX

$$E = \sum_{n=1}^{N} a_n \frac{e^{-jk_0R_n}}{\boldsymbol{R_n}} \cdot EF_n(\varphi) = \frac{e^{-jk_0r}}{r} \sum_{n=1}^{N} a_n e^{+jk_0 a sin\theta cos(\varphi-\varphi_n)} \cdot EF_n(\varphi), \quad (1)$$

where, $a_n = I_n e^{\alpha_n}$ are the element excitation and the distance R_n is approximated by r for the amplitude terms and by factor $r - asin\theta cos(\varphi - \varphi_n)$. Moreover, a is the distance between the two array elements. Thus the progressive phase shift is,

$$\alpha_n = -l_0 a sin\theta_0 cos(\phi_0 - \phi_n). \quad (2)$$

Magnetic current on vertical faces of the cube is given by,

$$\boldsymbol{M}(x', y', z') = \boldsymbol{a_z} M_0 sin\left[k\left(\frac{SL}{2} - |z'|\right)\right], \quad (3)$$

for $|z'| \leq \frac{GWZ}{2}$, $|y'| < \frac{SW}{2}$ and $x' = \frac{GW}{2}'$, where, $k = k_0\sqrt{\epsilon_r}$ is the wavenumber in the substrate and $\boldsymbol{a_z} M_0 = -2\boldsymbol{n} \times \boldsymbol{a_y} E_0$.

$$EF = E_\phi \boldsymbol{a_\phi} = j\frac{M_0 e^{-jkr}}{\pi r sin\theta} \times EY_{(\phi,\theta)} \times EZ_{(\theta)} \boldsymbol{a_\phi}, \quad (4)$$

where,

$$EY_{(\phi,\theta)} = \begin{cases} \frac{sin\left(k_y \frac{SW}{2}\right)}{K_y}, & -90 \leq \phi \leq 90 \\ 0, & 90 < \phi < 270, \end{cases} \quad (5)$$

$$EZ_{(\theta)} = cos\left(k_z \frac{GWZ}{2}\right) sin\left(k_0 \frac{GWZ}{2}\right) - sin\left(k_z \frac{GWZ}{2}\right) cos\left(k_0 \frac{GWZ}{2}\right) cos\theta \quad (6)$$

where, $k_x = k_0 sin\theta cos\phi$, $k_y = k_0\, sin\theta sin\phi$ and $k_z = k_0\, cos\theta$

$$\boldsymbol{EF_n(\varphi)} = \boldsymbol{EF}(|\phi - (n-1)90^\circ|) \quad (7)$$

where $(n-2)90^\circ \leq \phi \leq n90^\circ$ for $\phi_n = (n-1)90^\circ$

$$\boldsymbol{E} = \begin{cases} \boldsymbol{EF_1} \cdot e^{jkasin\theta cos(\phi - 0^\circ)} + \boldsymbol{EF_2} \cdot e^{jkasin\theta cos(\phi - 90^\circ)}, & 0^\circ \leq \phi \leq 90^\circ \\ \boldsymbol{EF_2} \cdot e^{jkasin\theta cos(\phi - 90^\circ)} + \boldsymbol{EF_3} \cdot e^{jkasin\theta cos(\phi - 180^\circ)}, & 90^\circ \leq \phi \leq 180^\circ \\ \boldsymbol{EF_3} \cdot e^{jkasin\theta cos(\phi - 180^\circ)} + \boldsymbol{EF_4} \cdot e^{jkasin\theta cos(\phi - 270^\circ)}, & 180^\circ \leq \phi \leq 270^\circ \\ \boldsymbol{EF_4} \cdot e^{jkasin\theta cos(\phi - 270^\circ)} + \boldsymbol{EF_1} \cdot e^{jkasin\theta cos(\phi - 0^\circ)}, & 270^\circ \leq \phi \leq 360^\circ. \end{cases} \quad (8)$$

$$\boldsymbol{E} = \boldsymbol{a_\phi} j\frac{M_0\, e^{-jkr}}{\pi r sin\theta} \times EZ_{(\theta)} \cdot \begin{cases} \boldsymbol{EY_{(\phi,\theta)}} \cdot e^{jkasin\theta cos(\phi - 0^\circ)} + \boldsymbol{EY_{(\phi - 90^\circ,\theta)}} \cdot e^{jkasin\theta cos(\phi - 90^\circ)}, & 0^\circ \leq \phi \leq 90^\circ \\ \boldsymbol{EY_{(\phi - 90^\circ,\theta)}} \cdot e^{jkasin\theta cos(\phi - 90^\circ)} + \boldsymbol{EY_{(\phi - 180^\circ)}} \cdot e^{jkasin\theta cos(\phi - 180^\circ)}, & 90^\circ \leq \phi \leq 180^\circ \\ \boldsymbol{EY_{(\phi - 180^\circ,\theta)}} \cdot e^{jkasin\theta cos(\phi - 180^\circ)} + \boldsymbol{EY_{(\phi - 270^\circ,\theta)}} \cdot e^{jkasin\theta cos(\phi - 270^\circ)}, & 180^\circ \leq \phi \leq 270^\circ \\ \boldsymbol{EY_{(\phi - 270^\circ,\theta)}} \cdot e^{jkasin\theta cos(\phi - 270^\circ)} + \boldsymbol{EY_{(\phi,\theta)}} \cdot e^{jkasin\theta cos(\phi - 0^\circ)}, & 270^\circ \leq \phi \leq 360^\circ. \end{cases} \quad (9)$$

$$\boldsymbol{E} = \boldsymbol{a_\phi} j\frac{M_0\, e^{-jkr}}{\pi r sin\theta} \times EZ_{(\theta)} \cdot \begin{cases} \frac{sin\left(k_0 sin\theta sin\phi \frac{SW}{2}\right)}{k_0 sin\theta sin\phi} e^{jkasin\theta cos(\phi)} + \frac{sin\left(k_0 sin\theta cos\phi \frac{SW}{2}\right)}{k_0 sin\theta cos\phi} e^{jkasin\theta sin(\phi)}, & 0^\circ \leq \phi \leq 90^\circ \\ \frac{sin\left(k_0 sin\theta cos\phi \frac{SW}{2}\right)}{k_0 sin\theta cos\phi} e^{jkasin\theta sin(\phi)} + \frac{sin\left(k_0 sin\theta sin\phi \frac{SW}{2}\right)}{k_0 sin\theta sin\phi} e^{-jkasin\theta cos(\phi)}, & 90^\circ \leq \phi \leq 180^\circ \\ \frac{sin\left(k_0 sin\theta sin\phi \frac{SW}{2}\right)}{k_0 sin\theta sin\phi} e^{jkasin\theta cos(\phi)} + \frac{sin\left(k_0 sin\theta cos\phi \frac{SW}{2}\right)}{k_0 sin\theta cos\phi} e^{jkasin\theta sin(\phi)}, & 180^\circ \leq \phi \leq 270^\circ \\ \frac{sin\left(k_0 sin\theta cos\phi \frac{SW}{2}\right)}{k_0 sin\theta cos\phi} e^{jkasin\theta sin(\phi)} + \frac{sin\left(k_0 sin\theta sin\phi \frac{SW}{2}\right)}{k_0 sin\theta sin\phi} e^{jkasin\theta cos(\phi)}, & 270^\circ \leq \phi \leq 360^\circ. \end{cases} \quad (10)$$

V. ACKNOWLEDGMENT

The authors would like to thank Rogers corporation for providing PCB materials samples and CMC for simulation software. Authors thank Payson system as well.

REFERENCES

[1] H. A. Damis, N. Khalid, R. Mirzavand, H.-J. Chung, and P. Mousavi, "Investigation of epidermal loop antennas for biotelemetry IoT applications," *IEEE Access*, vol. 6, pp. 15806–15815, 2018.

[2] C. Perera, C. H. Liu, S. Jayawardena, and M. Chen, "A survey on Internet of Things from industrial market perspective," *IEEE Access*, vol. 2, pp. 1660–1679, 2014.
[3] S. Shamsinejad, "3-D cubic slot antennas with application in wireless sensor networks," Ph.D. dissertation, Univ. Alberta, Edmonton, AB, Canada, 2017.
[4] Y. Yoshimura, "A microstripline slot antenna (Short Papers)," *IEEE Trans. Microw. Theory Techn.*, vol. MTT-20, no. 11, pp. 760–762, Nov. 1972.
[5] S. Muhamud-Kayat, M. T. Ali, M. K. M. Salleh, and M. H. M. Rusli, "Reconfigurable gap-coupled back-to-back truncated rhombus-like slotted patch antenna with steerable beams," in *Proc. 21st Int. Conf. Telecommun. (ICT)*, May 2014, pp. 338–342.
[6] V.-A. Nguyen, M.-H. Jeong, M.-T. Dao, and S.-O. Park, "Four-port beam reconfigurable antenna array for pattern diversity system," *IET Microwaves, Antennas Propag.*, vol. 6, no. 10, pp. 1179–1186, Jul. 2012.
[7] D. Patron, D. Piazza, and K. R. Dandekar, "Wideband planar antenna with reconfigurable omnidirectional and directional radiation patterns," *Electron. Lett.*, vol. 49, no. 8, pp. 516–518, Apr. 2013.
[8] S. Shamsinejad, F. De Flaviis, and P. Mousavi, "Microstrip-fed 3-D folded slot antenna on cubic structure," *IEEE Antennas Wireless Propag. Lett.*, vol. 15, pp. 1081–1084, 2016.
[9] S. Shamsinejad, F. M. Monavar, F. De Flaviis, G. Moradi, and P. Mousavi, "Three-dimensional-folded annular slot antenna-package," *Microw. Opt. Technol. Lett.*, vol. 59, no. 8, pp. 1871–1876, Aug. 2017.
[10] X. Yi, L. Huitema, and H. Wong, "Polarization and pattern reconfigurable cuboid quadrifilar helical antenna," *IEEE Trans. Antennas Propag.*, vol. 66, no. 6, pp. 2707–2715, Jun. 2018.
[11] S. I. H. Shah, M. M. Tentzeris, and S. Lim, "Low-cost circularly polarized origami antenna," *IEEE Antennas Wireless Propag. Lett.*, vol. 16, pp. 2026–2029, 2017.
[12] J. Sarrazin, Y. Mahe, S. Avrillon, and S. Toutain, "Pattern reconfigurable cubic antenna," *IEEE Trans. Antennas Propag.*, vol. 57, no. 2, pp. 310–317, Feb. 2009.
[13] S. Shamsinejad and P. Mousavi, "Pattern reconfigurable multimode square waveguide slot antenna," in *Proc. IEEE Int. Symp. Antennas Propag. (APSURSI)*, Jun./Jul. 2016, pp. 1315–1316.
[14] T. M. Weller, L. P. B. Katehi, and G. M. Rebeiz, "Single and double folded-slot antennas on semi-infinite substrates," *IEEE Trans. Antennas Propag.*, vol. 43, no. 12, pp. 1423–1428, Dec. 1995.
[15] J. Volakis, *Antenna Engineering Handbook*, 4th ed. New York, NY, USA: McGraw-Hill, 2007.
[16] A. B. Constantine, *Antenna Theory: Analysis and Design*, 3rd ed. Hoboken, NJ, USA: Wiley, 2005.
[17] L. Josefsson and P. Persson, *Conformal Array Antenna Theory and Design*, vol. 29. Hoboken, NJ, USA: Wiley, 2006.
[18] M. Sanad, "Microstrip antennas on very small ground planes for portable communication systems," in *Proc. IEEE Antennas Propag. Soc. Int. Symp.*, vol. 2, Jun. 1994, pp. 810–813.
[19] F. Sabath, M. Bucker, and S. Oing, "Influence of finite ground planes on the transmission line current distribution," *IEEE Trans. Magn.*, vol. 32, no. 3, pp. 1501–1504, May 1996.
[20] S. Maci, L. Borselli, and A. Cucurachi, "Diffraction from a truncated grounded dielectric slab: A comparative full-wave/physical-optics analysis," *IEEE Trans. Antennas Propag.*, vol. 48, no. 1, pp. 48–57, Jan. 2000.
[21] M. Jusoh, T. Sabapathy, M. F. Jamlos, and M. R. Kamarudin, "Reconfigurable four-parasitic-elements patch antenna for high-gain beam switching application," *IEEE Antennas Wireless Propag. Lett.*, vol. 13, pp. 79–82, 2014.

SOUREN SHAMSINEJAD (S'12) received the B.Sc. degree in electrical engineering from the Amirkabir University of Technology (Tehran Polytechnic), Tehran, Iran, in 2004, and the M.Sc. degree in electrical engineering (communications-fields and waves) from the Iran University of Science and Technology, Tehran, in 2007. He is currently pursuing the Ph.D. degree in electrical engineering (electromagnetics and microwave) with the University of Alberta, Edmonton, AB, Canada.

His current research interests include active integrated antennas, intelligent small antennas, RF, and optical MEMS.

Mr. Shamsinejad was a recipient of the NSERC Industrial Postgraduate Scholarship and the Alberta Innovates-Technology Future Graduate Student Scholarship.

NABIL KHALID (S'15) received the bachelor's degree in electrical engineering from Air University, Islamabad, Pakistan, in 2013, with majors involved telecommunications, RF/Microwave, and RADARs, and the M.Sc. degree in electrical and computer engineering from Koc University, Istanbul, Turkey, with the focus on developing the physical layer of THz Band wireless communications. He is currently pursuing the Ph.D. degree under the supervision of Prof. P. Mousavi with the Electrical and Computer Engineering Department, University of Alberta, Edmonton, Canada, with the focus on designing efficient MIMO antennas. He was with RWR Pvt. Ltd., Islamabad, Pakistan, from 2013 to 2014, as a Design Engineer with the RF/Microwave Department. His focus was on designing industrial grade power amplifiers. From 2015 to 2017, he was with the Next-generation and Wireless Communications Laboratory (NWCL) as a Research Assistant. He joined the Intelligent Wireless Technologies Laboratory (IWT) as a Research Assistant, in 2017.

FATEMEH M. MONAVAR (S'12) received the B.Sc. degree in biomedical engineering (bioelectric) from the Amirkabir University of Technology (Tehran Polytechnic), Tehran, Iran, in 2006, and the M.Sc. degree in electrical engineering (communications-fields and waves) from the Iran University of Science and Technology, Tehran, in 2010. She is currently pursuing the Ph.D. degree in electrical engineering (electromagnetics and microwave) with the University of Alberta, Edmonton, AB, Canada.

Her current research interest includes antenna analysis and design.

Ms. Monavar was a recipient of the NSERC Industrial Postgraduate Scholarship and the Queen Elizabeth II Graduate Scholarship-Doctoral level.

SHILA SHAMSADINI is currently pursuing the Ph.D. degree and a Research Assistant with the Integrated Circuits and Systems (iCAS) Laboratory, ECE Department, University of Alberta, Canada.

RASHID MIRZAVAND (M'12–SM'16) received the B.Sc. degree from the Isfahan University of Technology, Isfahan, Iran, in 2004, and the M.Sc. and Ph.D. degrees from the Amirkabir University of Technology (Tehran Polytechnic), Tehran, Iran, in 2007 and 2011, respectively, all in electrical engineering.

Since 2011, he has been a Research Professor with the Amirkabir University of Technology. He is currently a Research Associate with the Intelligent Wireless Technology Laboratory, University of Alberta, Edmonton, AB, Canada. He has authored more than 85 papers published in refereed journals and conferences proceedings. His research interests include integrated sensors and microwave/millimeter-wave circuits.

Dr. Mirzavand received the Best Ph.D. Thesis Award from the Amirkabir University of Technology, in 2012, the Best National ICT Researcher Award from the Ministry of Information and Communications Technology of Iran, in 2013, the Elite Young Researcher Grant Award from Iran's NEF, in 2014, and the Alberta Innovates Technology Futures Elite Postdoctoral Fellowship Award, in 2015.

GHOLAMREZA MORADI (M'09–SM'16) was born in Shahriar, Iran, in 1966. He received the B.Sc. degree in electrical communication engineering from Tehran University, Tehran, Iran, in 1989, the M.Sc. degree in electrical communication engineering from the Iran University of Science and Technology, Tehran, in 1993, and the Ph.D. degree in electrical engineering from Tehran Polytechnic University, Tehran, in 2002. From 1997 to 2006, he was a Faculty Member with the Civil Aviation Technology College, Tehran. In 2003, he was selected as an Exemplary Researcher of the Iranian Ministry of Road and Transportation. He is currently an Associate Professor with the Department of Electrical Engineering, Amirkabir University of Technology (Tehran Polytechnic), Tehran. He has authored or coauthored several papers in refereed journals and local and international conferences. He has coauthored *Communication Transmission Lines* [Nahr-e-Danesh Press, 2007 (in Persian)], *Active Transmission Lines* [Amirkabir University Press, 2008 (in Persian)], and *Microwave Engineering* [Nahr-e-Danesh Press, 2008 (in Persian)]. His main research interests include numerical electromagnetics, antennas, and active microwave, and millimeter-wave circuits and systems.

PEDRAM MOUSAVI (M'00–SM'14) received the B.Sc. degree (Hons.) in telecommunication engineering from the Iran University of Science and Technology, Tehran, in 1995, and the M.Sc. and Ph.D. degrees from the University of Manitoba, Winnipeg, Canada, in 1997 and 2001, respectively, all in electrical engineering.

He is currently a Professor with the Department of Mechanical Engineering and a NSERC-AI Industrial Research Chair in intelligent integrated sensors and antennas with the University of Alberta. His current mission is to foster a strong collaboration between industry and academia and stimulate more industry relevant research in wireless technologies. The research conducted through this industrial chair program will allow information and communications technology (ICT) innovations to be applied to the areas of intelligent integrated sensors and antennas to improve the productivity of the oil-energy sector and to sustain its growth. He has more than 180 refereed journal and conference articles and several patents in this field. His research interests include advanced intelligent antenna, microwave and millimeter-waves circuits and systems, 5G phased array antennas, UWB radar systems, 3-D printing electronics, and the Zero-power IoT.

Dr. Mousavi has over fifteen years of entrepreneurial academic experience with start-up companies from the University of Waterloo and the University of Alberta. He founded Intelwaves Technologies as a spin-off from the University of Waterloo. He is a Co-Founder of WiDyne Technologies and SenZioT Technologies from the University of Alberta.